

## Nanoscale mechanical behavior of individual semiconducting nanobelts

Scott X. Mao<sup>a)</sup> and Minhua Zhao

*Department of Mechanical Engineering, University of Pittsburgh, Pittsburgh, Pennsylvania 15261*

Zhong Lin Wang

*School of Materials Science and Engineering, Georgia Institute of Technology, Atlanta, Georgia 30332-0245*

(Received 7 April 2003; accepted 2 June 2003)

Nanobelts are a group of materials that have a rectangle-like cross section with typical widths of several hundred nanometers, width-to-thickness ratios of 5–10, and lengths of hundreds of micrometers. In this letter, nanoindentations were made in individual ZnO and SnO<sub>2</sub> nanobelts by a cube corner diamond indenter. It is shown that the effect of indentation size is still obvious for indentation depths less than 50 nm. It is also demonstrated that nanomachining of nanobelts is possible using an atomic force microscope tip. © 2003 American Institute of Physics.  
[DOI: 10.1063/1.1597754]

In recent years, quasioone-dimensional (1D) solid nanostructures (nanowires and nanobelts) have stimulated considerable interest for scientific research due to their importance in mesoscopic physics studies and their potential applications. Compared to micrometer diameter whiskers and fibers, these nanostructures are expected to have remarkable optical, electrical, magnetic, and mechanical properties. Exploration of novel methods for large-scale synthesis of 1D nanostructures is a challenging area of research. As *n*-type semiconductive materials, zinc oxide (ZnO) has received a considerable amount of attention over the last few years because of its many applications in various fields. ZnO is now widely used as an transparent conducting oxide material and gas sensor.<sup>1</sup>

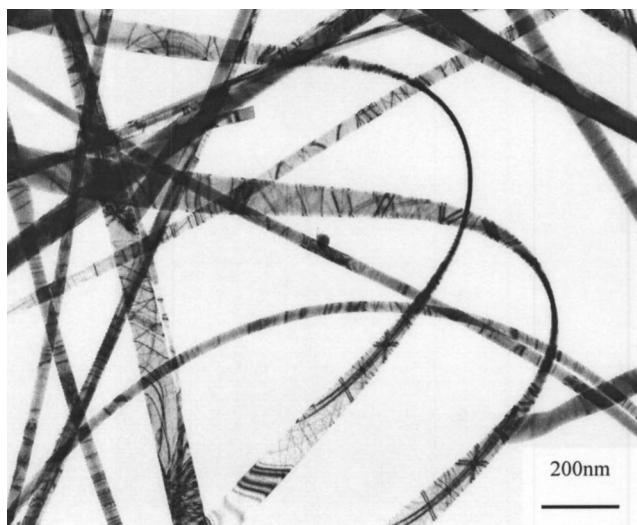
Recently, Wang and co-workers<sup>2–4</sup> have synthesized belt-like oxides (so-called nanobelts) by evaporating ZnO or SnO<sub>2</sub> powder at high temperatures without the presence of a catalyst. The belt-like morphology is distinct from that of semiconductor nanowires. With well-defined geometry and perfect crystallinity, semiconducting oxide belts are likely to be a model material family for understanding mechanical behavior at the nanoscale in the absence of dislocations and defects (excluding point defects). The dimension of the nanobelt as a mechanical cantilever potentially can be used as a mechanical resonator<sup>5</sup> or as an electro-optical resonator.<sup>6</sup> Since a nanobelt can be used as a nanomechanical device, it is important to measure its mechanical behavior. In this study, nanoscale mechanical properties of individual zinc oxide nanobelts were characterized by the Nanoscope IIIa atomic force microscope (AFM) and the Hysitron TriboScope with a homemade side view charge coupled device (CCD) camera. It showed that the effect of indentation size was still obvious for indentation depth less than 50 nm. It also demonstrated that nanomachining of nanobelts is possible using an AFM tip.

The synthesis of nanobelts was based on thermal evaporation of oxide powders under controlled conditions without the presence of a catalyst.<sup>2–4</sup> The procedures for preparing

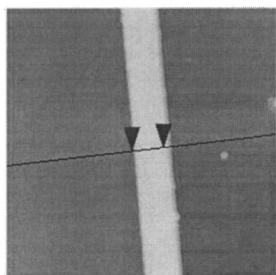
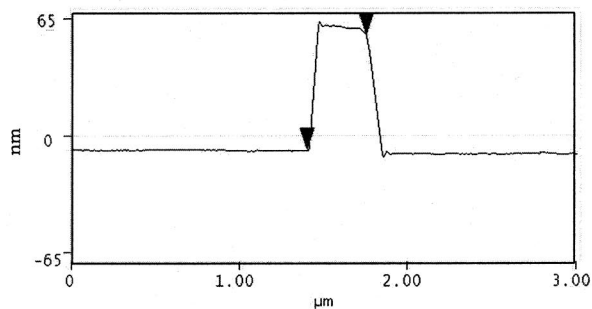
dispersed nanobelts for the study reported here are as follows:<sup>7–8</sup> first immerse wool-like nanobelts in acetone, and disperse the mixture by an ultrasonic cleaning device. Then dip the polished silicon wafer into the solution and pull it out. After drying, a single nanobelt was placed on a silicon substrate. The nanobelt sample prepared was investigated using a diamond cube corner tip (including the 90° angle of a three sided pyramid) with nominal radius of 40 nm. Individual nanobelts were imaged before and after nanoindentation.

Figure 1(a) is a transmission electron microscopy (TEM) picture of ZnO nanobelts showing their geometrical shape. Some of them are straight and some twisted, displaying shape characteristics of the belts. The nanobelt was grown along the [0001] direction and enclosed by {10 $\bar{1}$ 0} facets.<sup>2</sup> Section analysis by atomic force microscope in Fig. 1(b) shows the nanobelt has a rectangular section. The width of the nanobelt is about 360 nm and the height is about 65 nm. This gives a width-to-thickness ratio of 5.5. These values are typical of a single nanobelt. After lying on a silicon substrate, the nanobelt was indented by a cubic indenter under AFM as shown in Fig. 2. The load is 0–300  $\mu$ N with a loading rate of 10  $\mu$ N/s. Using the method of Oliver and Pharr,<sup>9</sup> the hardness of the ZnO and SnO<sub>2</sub> nanobelts on (2 $\bar{1}$  $\bar{1}$ 0) and (10 $\bar{1}$ ), surfaces respectively, was calculated as a function of indentation penetration. Although no pile-up effect<sup>10</sup> was taken into consideration here, it is a minor problem for indentation that is very shallow (less than 50 nm) and material that is ceramic. It can be seen from Fig. 3 that both the ZnO and SnO<sub>2</sub> nanobelts show marked ISE for less than 50 nm indentation, which can be attributed to the effect of the strain gradient during nanoindentation of metallic or ceramic materials.<sup>11–17</sup> Less penetration of nanoindentation gives a higher strain gradient in the material under the indentation area based on experimental measurement.<sup>18</sup> Flow stress under the indentation is dependent on not only deformation strain but also on the strain gradient. The strain gradient will increase the flow stress based on strain gradient theory.<sup>11,12,19–21</sup> Therefore, the strain gradient induced by less penetration will increase the flow stress and consequently the hardness of the nanobelts. The scatter in testing

<sup>a)</sup>Author to whom correspondence should be addressed; electronic mail: smao@enr.pitt.edu



(a)



(b)

FIG. 1. (a) TEM picture of ZnO nanobelts showing their geometrical shape (after Ref. 2). Some of them are straight and some twisted. (b) AFM section analysis showing the nanobelt has a rectangular section.

data is due to surface conditions such as the effect of roughness on shallow indentation. The typical roughness was less than 2 nm root mean square (rms) over 1  $\mu\text{m}^2$ .

Comparison of the ZnO nanobelt with a ZnO bulk (0001) single crystal was carried out by nanoindentation. As shown in Fig. 4, the ZnO nanobelt is a little softer than the bulk single crystal. This is likely due to the fact that (0001) is the most closely packed plane for hexagonal structured ZnO. Thus, the hardness along [0001] (the  $c$  axis) may be higher than that along  $[2\bar{1}10]$  (the  $a$  axis), which is the normal direction of the nanobelt.

A nanoindentation induced fracture test for SnO<sub>2</sub> was also carried out by a cantilever type AFM diamond indenter with nominal radius of 25 nm. Figure 5(a) shows a crack

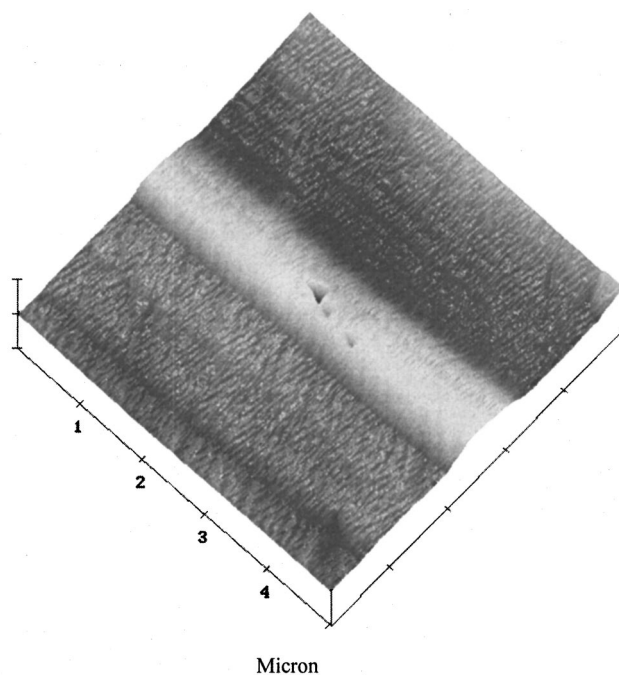


FIG. 2. Indentation of a SnO<sub>2</sub> nanobelt by a cubic indenter. The load for large and small indents is 300 and 200  $\mu\text{N}$ , respectively.

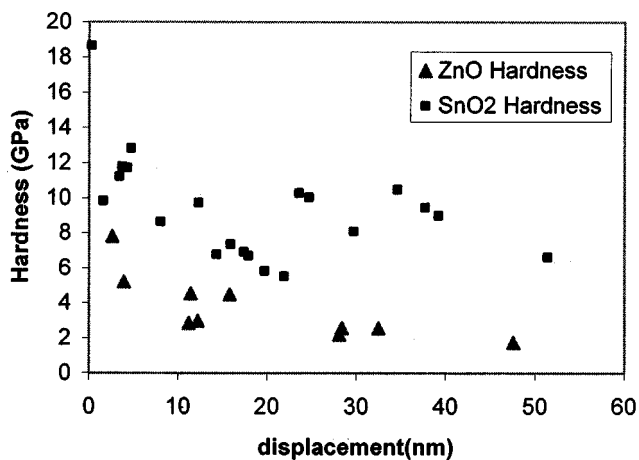


FIG. 3. Hardness of ZnO and SnO<sub>2</sub> nanobelts as a function of penetration during nanoindentation.

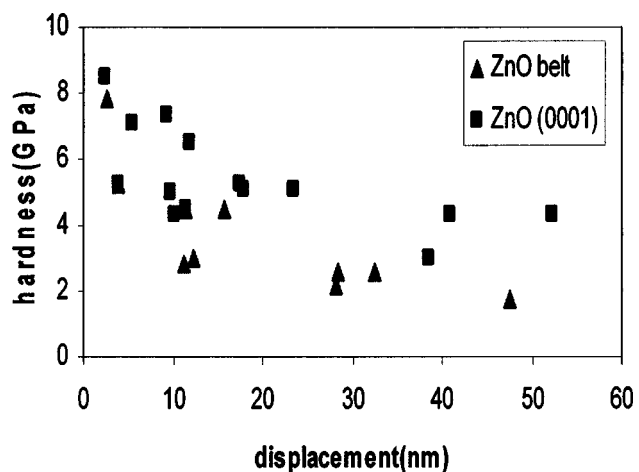
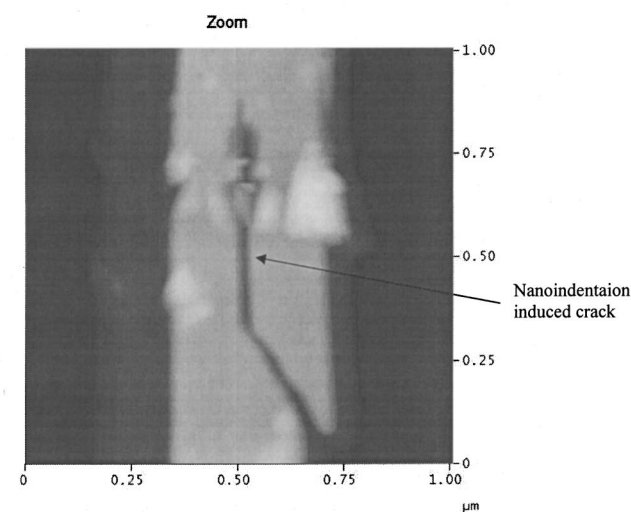
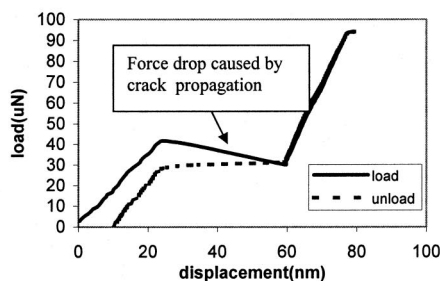


FIG. 4. Hardness of a ZnO nanobelt and bulk single crystal (0001).



(a)



(b)

FIG. 5. Crack nucleation and propagation in a  $\text{SnO}_2$  nanobelt by nanoindentation under AFM: (a) crack induced by nanoindentation and (b) indentation load vs. penetration curve which indicates unstable crack propagation.

induced by nanoindentation, which was initiated from a triangular edge of the indenter. The crack propagates along  $[101]$ , and the cleavage surface is  $(010)$  based on structural information provided by electron microscopy.<sup>2</sup> Figure 5(b) shows the indentation load versus penetration curve, which indicates unstable crack propagation when  $43 \mu\text{N}$  indentation load is applied. This is probably the load at which the crack is created. After penetration reaches  $60 \text{ nm}$  ( $\sim$  the belt thickness), the nanoindenter starts, indenting the Si substrate

and the load starts picking up since the Si substrate is harder than the  $\text{SnO}_2$  crystal. The fracture test for  $\text{SnO}_2$  demonstrated the possibility of cutting or machining the nanobelt down to a smaller size under AFM.

In summary, imaging, manipulating, and testing of mechanical properties of a single nanobelt of ZnO and  $\text{SnO}_2$ , whose size is in the nano- to micrometer range, were performed under an atomic force microscope. The hardness of the ZnO nanobelt is less than that of  $\text{SnO}_2$  and both show obvious ISE for less than  $50 \text{ nm}$  indentation. Furthermore, the hardness along  $[2\bar{1}\bar{1}0]$  ( $a$  axis) on  $(01\bar{1}0)$  of the dislocation free ZnO nanobelt is slightly less than that of the  $c$ -axis oriented bulk  $(0001)$  ZnO single crystal.

The authors are grateful for support from NSF Grant No. CMS-0140317 to University of Pittsburgh and NSF Grant No. DMR-9733160 to Georgia Tech.

- <sup>1</sup>M. S. Arnold, P. Avouris, Z. W. Pan, Z. L. Wang, and T. J. Watson (unpublished).
- <sup>2</sup>Z. W. Pan, Z. Dai, and Z. L. Wang, *Science* **291**, 1947 (2001).
- <sup>3</sup>Z. R. Dai, Z. W. Pan, and Z. L. Wang, *Solid State Commun.* **118**, 351 (2001).
- <sup>4</sup>Z. W. Pan, Z. R. Dai, and Z. L. Wang, *Appl. Phys. Lett.* **80**, 309 (2002).
- <sup>5</sup>P. Poncharal, Z. L. Wang, D. Ugarte, and W. A. de Heer, *Science* **283**, 1516 (1999).
- <sup>6</sup>H. Kind, H. Yan, B. Messer, M. Law, and P. Yang, *Adv. Mater. (Weinheim, Ger.)* **14**, 16 (2002).
- <sup>7</sup>M. Zhao, S. Mao, F. Xu, J. A. Barnard, and Z. L. Wang, *Materials Research Society Fall Symposium, Boston, 2–6 December 2002*.
- <sup>8</sup>S. Mao, M. Zhao, and Z. L. Wang, in Ref. 7.
- <sup>9</sup>W. C. Oliver and G. M. Pharr, *J. Mater. Res.* **7**, 1564 (1992).
- <sup>10</sup>Y. Y. Lim, M. M. Chaudhri, and Y. Enomoto, *J. Mater. Res.* **14**, 2314 (1999).
- <sup>11</sup>N. A. Fleck, G. M. Muller, M. F. Ashby, and J. W. Hutchinson, *Acta Metall. Mater.* **42**, 475 (1994).
- <sup>12</sup>W. D. Nix and H. Gao, *J. Mech. Phys. Solids* **46**, 411 (1998).
- <sup>13</sup>N. A. Fleck and J. W. Hutchinson, *J. Mech. Phys. Solids* **49**, 2245 (2001).
- <sup>14</sup>N. A. Fleck and J. W. Hutchinson, *J. Mech. Phys. Solids* **141**, 1825 (1993).
- <sup>15</sup>N. A. Fleck and J. W. Hutchinson, *Advances in Applied Mechanics* (Academic, New York, 1997), Vol. 33, p. 295.
- <sup>16</sup>D. M. Duan, N. Wu, W. S. Slaughter, and S. X. Mao, *Mater. Sci. Eng., A* **303**, 241 (2001).
- <sup>17</sup>D. Duan, N. Wu, M. Zhao, W. S. Slaughter, and S. X. Mao, *J. Eng. Mater. Technol.* **124**, 167 (2002).
- <sup>18</sup>M. Zhao, W. S. Slaughter, M. Li, and S. X. Mao, *Acta Mater.* (in press).
- <sup>19</sup>E. W. Andrews, A. E. Giannakopoulos, E. Plisson, and S. Suresh, *Int. J. Solids Struct.* **39**, 281 (2002).
- <sup>20</sup>M. Dao, N. Chollacoop, K. J. Van Vliet, T. A. Venkatesh, and S. Suresh, *Acta Mater.* **49**, 3899 (2001).
- <sup>21</sup>M. F. Ashby, *Philos. Mag.* **21**, 399 (1970).